ACCOUNTS of chemical research

Article

pubs.acs.org/accounts

# Live-Cell Bioorthogonal Chemical Imaging: Stimulated Raman Scattering Microscopy of Vibrational Probes

Lu Wei,[†] Fanghao Hu,[†] Zhixing Chen,[†] Yihui Shen,[†] Luyuan Zhang,[†] and Wei Min*[,†,‡]

[†]Department of Chemistry, Columbia University, New York, New York 10027, United States

[‡]Kavli Institute for Brain Science, Columbia University, New York, New York 10027, United States

**CONSPECTUS:** Innovations in light microscopy have tremendously revolutionized the way researchers study biological systems with subcellular resolution. In particular, fluorescence microscopy with the expanding choices of fluorescent probes has provided a comprehensive toolkit to tag and visualize various molecules of interest with exquisite specificity and high sensitivity. Although fluorescence microscopy is currently the method of choice for cellular imaging, it faces fundamental limitations for studying the vast number of small biomolecules. This is because common fluorescent labels, which are relatively bulky, could introduce considerable perturbation to or even completely alter the native functions of vital small biomolecules. Hence, despite their immense functional importance, these small biomolecules remain largely undetectable by fluorescence microscopy.

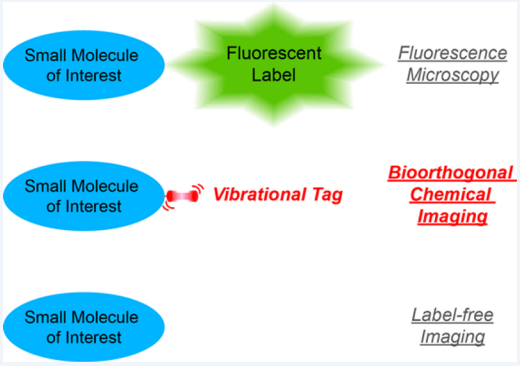


To address this challenge, a *bioorthogonal chemical imaging* platform has recently been introduced. By coupling stimulated Raman scattering (SRS) microscopy, an emerging nonlinear Raman microscopy technique, with tiny and Raman-active vibrational probes (e.g., alkynes and stable isotopes), bioorthogonal chemical imaging exhibits superb sensitivity, specificity, and biocompatibility for imaging small biomolecules in live systems. In this Account, we review recent technical achievements for visualizing a broad spectrum of small biomolecules, including ribonucleosides and deoxyribonucleosides, amino acids, fatty acids, choline, glucose, cholesterol, and small-molecule drugs in live biological systems ranging from individual cells to animal tissues and model organisms. Importantly, this platform is compatible with live-cell biology, thus allowing real-time imaging of small-molecule dynamics. Moreover, we discuss further chemical and spectroscopic strategies for *multicolor* bioorthogonal chemical imaging, a valuable technique in the era of "omics".

As a unique tool for biological discovery, this platform has been applied to studying various metabolic processes under both physiological and pathological states, including protein synthesis activity of neuronal systems, protein aggregations in Huntington disease models, glucose uptake in tumor xenografts, and drug penetration through skin tissues. We envision that the coupling of SRS microscopy with vibrational probes would do for small biomolecules what fluorescence microscopy of fluorophores has done for larger molecular species.

## 1. INTRODUCTION

Light microscopy, in particular, fluorescence microscopy, has been a powerful tool for researchers to study living systems at the microscopic level.[1,2] However, there remains a fundamental limitation for fluorescence imaging of small biomolecules, such as nucleosides, amino acids, fatty acids, choline, glucose, cholesterol, and small-molecule drugs, in living systems. This is because most small biomolecules are intrinsically nonfluorescent. However, if using fluorescent tagging, fluorescent probes such as organic dyes, fluorescent proteins, or quantum dots are all relatively bulkier in size than small biomolecules, thus often severely compromising the native biochemical or biophysical properties of these fluorophore-labeled small biomolecules inside live cells. Therefore, optical imaging methods offering molecular contrasts other than fluorescence are needed to study these small chemical species.

Raman microscopy presents an alternative for this purpose. Based on vibrational spectroscopy without the need for bulky fluorophore labeling, Raman imaging holds the promise for probing small molecules.[3] However, spontaneous Raman scattering (Figure 1a) is notoriously feeble, needing long acquisition time, and is vulnerable to sample autofluorescence. As a result, conventional Raman microscopy is a less-than-ideal bioimaging modality, especially for applications demanding high sensitivity, fast speed, deep tissue penetration, or correlative fluorescence and Raman imaging.[4,5] An advanced Raman technique, surface enhanced Raman scattering (SERS), could provide much higher sensitivity. Nevertheless, its reliance on metallic nanostructures limits its ability to probe small intracellular biomolecules.[6]

Partially overcoming both the sensitivity and biocompatibility issues, coherent anti-Stokes Raman scattering (CARS) microscopy offers an imaging speed close to fluorescence

Received: May 2, 2016
Published: August 3, 2016





DOI: 10.1021/acs.accounts.6b00210
Acc. Chem. Res. 2016, 49, 1494−1502

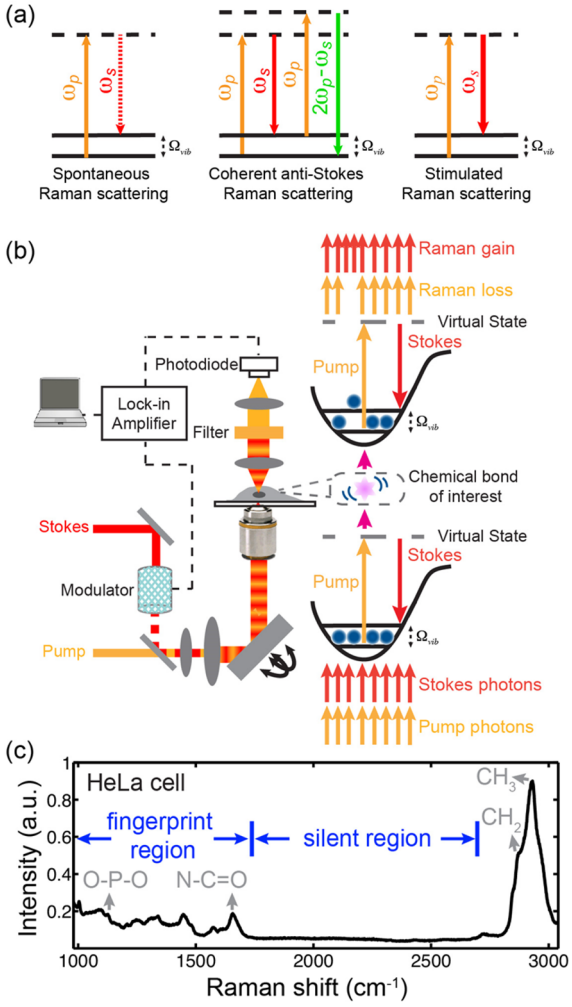


**Figure 1.** Physical principle and instrumental setup for stimulated Raman scattering microscopy. (a) Energy diagrams for spontaneous Raman scattering, coherent anti-Stokes Raman scattering (CARS), and stimulated Raman scattering (SRS). (b) Experimental setup of typical SRS microscopy. (c) Raman spectrum of mammalian cell samples designating the crowded fingerprint region and the cell-silent region.

microscopy by virtue of coherent amplification (Figure 1a).[7] Unfortunately, CARS microscopy suffers from spectral distortion, unwanted nonresonant background and non-straightforward concentration dependence.[8,9] Although some of these limitations can be addressed by advanced CARS derivatives, substantial technical complexity has to be involved.[8,10]

More recently, stimulated Raman scattering (SRS) microscopy emerged to complement and even supersede CARS in almost all aspects (Figure 1a).[11−17] Spectroscopically, the SRS spectrum is identical to that of spontaneous Raman without the complication of nonresonant background, thus offering straightforward and robust spectral interpretations.[12,18] The detection sensitivity of SRS readily approaches the shot-noise limit by taking advantage of the high-frequency modulation transfer scheme.[15,17] In addition, SRS signals are strictly linearly dependent on analyte concentrations, allowing for quantitative analysis. Moreover, the nonlinear nature and the adoption of near-infrared laser wavelengths allow SRS 3D optical sectioning into deep tissues.

In the most popular narrow-band excitation scheme, SRS microscopy utilizes two spatially and temporally synchronized picosecond laser pulse trains (pump and Stokes).[12,14−17] When the energy gap between two lasers is resonant with the vibrational level of targeted chemical bonds, the joint action of the pump and Stokes fields stimulates (i.e., accelerates) the otherwise slow vibrational transition by $10^8$ times.[15,17] Whenever a molecule is promoted into the vibrational excited state, the Stokes pulse gains a photon, whereas the pump pulse loses one (Figure 1b). By modulating the Stokes beam (or the pump beam) intensity at a high frequency (~megahertz) and detecting the resulting stimulated Raman loss (or gain) of the pump beam (or the Stokes beam) with a photodiode fed to a lock-in amplifier referenced at the same frequency as the modulation, shot-noise-limited high detection sensitivity is achieved, circumventing the laser intensity fluctuations occurring at low frequencies[12,15] (Figure 1b). After raster-scanning across the sample, one can produce a 3D concentration map of the targeted chemical bonds.

## 2. LABEL-FREE CHEMICAL IMAGING

Since the invention of the narrow-band SRS microscopy,[12] label-free imaging has been a central theme of its applications. A variety of molecular species have been imaged by label-free SRS targeting their intrinsic chemical bonds at the crowded cellular fingerprint region (500−1700 $cm^{-1}$) or the high frequency C−H or O−H region (2800−3200 $cm^{-1}$). Chemical bonds frequently probed are O−P−O, N−C═O, C═C, S═O, O−H, C−$H_2$, and C−$H_3$ (Figure 1c). Notable examples include (but are not limited to) monitoring DMSO and retinoic acid diffusion through skins of living mice and human,[12] video-rate imaging for skin samples,[14] imaging nucleic acids *in vivo*,[19] delineating tumor margins,[20] tracking changes of lipid composition,[21] imaging intracellular drug distribution in living cells[22] and detecting membrane potential.[23] The success of these label-free applications has inspired developments in spectroscopic imaging and will continue to generate a profound impact in biomedicine.[17]

Despite the popularity of label-free imaging for biomedicine, this strategy has a few limitations. First, the detection specificity is usually compromised. It is rather difficult to distinguish a target biomolecule from the sea of the other related species inside cells since the differentiable vibrational signatures are finite and many biomolecular species share similar chemical bonds.[24] Second, the Raman scattering cross sections of the endogenous chemical bonds are usually limited. The resulting detection sensitivity of label-free SRS is often in the range of millimolar, not sensitive enough for capturing the activities of many interesting small biomolecules.[15] Third, although the label-free approach is highly powerful for stationary imaging, it usually lacks the ability for probing dynamic metabolism including uptake, trafficking, and turnover of small biomolecules. Therefore, there is a strong need for conceptual innovations to go beyond the label-free strategy to further boost specificity and sensitivity, as well as to probe dynamics.

## 3. BIOORTHOGONAL CHEMICAL IMAGING: SRS MICROSCOPY OF VIBRATIONAL PROBES

The concept of vibrational probes has been around in the field of vibrational spectroscopy.[25] Indeed, nitriles (C≡N) and carbonyls (C═O) are used to probe local electrostatics and dynamics in proteins and enzymes through the vibrational Stark


DOI: 10.1021/acs.accounts.6b00210
*Acc. Chem. Res.* 2016, 49, 1494−1502

effect.[26] Evolving from spectroscopy to microscopy, the idea of detecting vibrational probes leads to the initial demonstrations of spontaneous Raman imaging of Raman active probes including stable isotopes (Huang et al.[27] and van Manen et al.[28]) and alkynes, that is, C≡C, (Yamakoshi et al.[29,30]) inside cells and SERS imaging of bioorthogonal Raman reporter on cell surface (Lin et al.[31]). Among the probes, alkynes stand out as widely exploited small molecule handles for imaging and identification in the booming field of *bioorthogonal chemistry*.[32−38] Inspired by these previous efforts and success, a general *bioorthogonal chemical imaging* platform has recently emerged by coupling SRS microscopy with tiny vibrational probes.[39−50] Such an optical imaging scheme presents a hybrid strategy between the conventional fluorescence microscopy and the label-free vibrational imaging approach, thereby offering the desired combination of high detection sensitivity and specificity, minimal perturbations, and dynamical analysis capacity.

Specifically, three distinct classes of bioorthogonal vibrational probes were explored: alkyne (C≡C) moieties, deuterium isotope, and $^{13}C$ isotope. Physically, unlike the bulky fluorophores, these probes consist of only several atoms, thus exerting little perturbation to the native function of small biomolecules. Spectroscopically, both C≡C (as well as C≡N) carbon-deuterium bonds exhibit Raman peaks at the cell-silent region where no other peaks from endogenous molecules exist (Figure 1c), achieving exquisite detection specificity. Biochemically, these probes are generally absent (or at extremely low abundance) inside cells, and are inert to cellular reactions or exchanges. Hence, SRS imaging of these vibrational probes, which are both spectroscopically and biochemically orthogonal to the endogenous molecules inside cells, is termed bioorthogonal chemical imaging. Such a platform is well suited for probing small-molecule dynamics in living systems with high spatial and temporal resolution. We herein summarize and discuss the most recent advances toward this front.

## 4. SRS IMAGING OF ALKYNES FOR VISUALIZING SMALL BIOMOLECULES WITH HIGH SENSITIVITY

Alkynes possess desirable features for tagging a wide variety of small biomolecules with subsequent imaging by SRS microscopy. Chemically, they are small (only two atoms), bioorthogonal, and easy to install.[32−38] Spectroscopically, the stretching motion of C≡C presents a substantial change of polarizability, displaying a sharp and strong Raman peak around 2125 $cm^{-1}$ in the cell-silent region.[24] In fact, Raman scattering cross sections of alkynes are higher than almost all the endogenous chemical bonds in label-free imaging. The reported SRS detection limit for alkynes is down to 200 $\mu$M under a 100 $\mu$s acquisition time in 5-ethynyl-2′-deoxyuridine (EdU), an alkyne-tagged thymidine analog,[39] much more sensitive than previous label-free SRS reports in the millimolar range.[12]

Although alkynes have been heavily explored as imaging and identification handles in bioorthogonal chemistry,[32−38] clearly proving their minimal toxicity and high biocompatibility *in vivo*, the subsequent visualization by click-reaction between alkyne-tagged molecules and azide-tagged fluorophores normally involves the catalysis of copper(I) ion, which is toxic to live cells. Even for the latest copper-free version, the reaction has nonideal kinetics and is often associated with high background originated from nonspecific staining.[51] Moreover, it is a nontrivial task to homogeneously deliver these fluorophores to live tissues and animals. To this end, direct SRS imaging of alkyne-tagged small molecules is free from all these complications by bypassing the click reaction and the fluorophores altogether.

Wei et al. in 2014 first demonstrated SRS imaging for a broad spectrum of alkyne-tagged small-molecule building blocks, including deoxyribonucleosides, ribonucleosides, amino acids, choline, and fatty acids (Figure 2a) for the *de novo* synthesis of

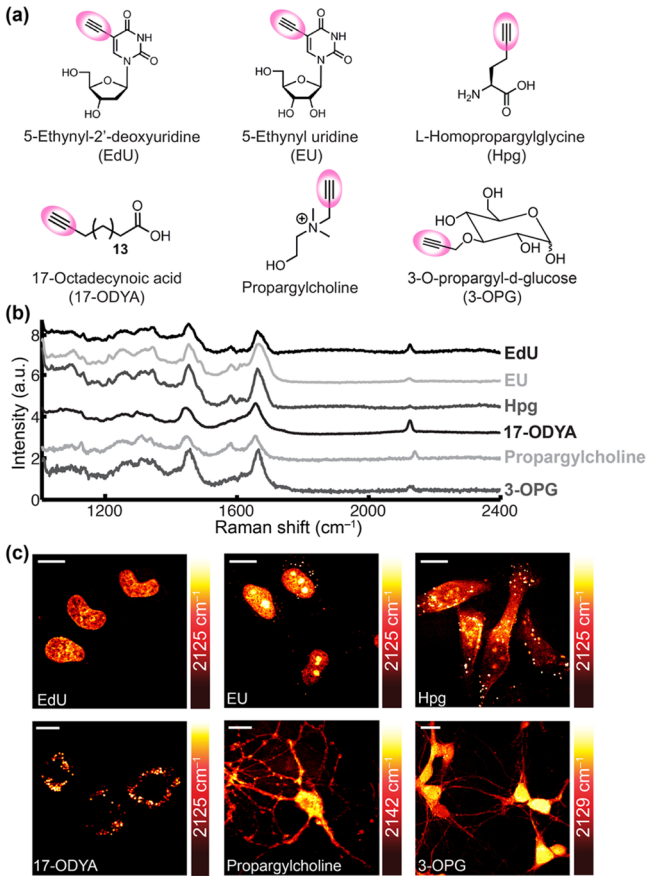


**Figure 2.** Sensitive and specific SRS imaging for diverse alkyne-bearing small biomolecules. (a) Chemical structures of alkyne-tagged small biomolecules. (b,c) The corresponding spontaneous Raman spectra (b) and the SRS images (c) of each alkyne-tagged small biomolecule after metabolic incorporation into mammalian cells or neurons. Adapted from refs 39 and 41. Copyright 2014 Nature Publishing Group and Copyright 2015 John Wiley & Sons, Inc. Scale bar: 10 $\mu$m.

DNA, RNA, proteome, triglycerides, and phospholipids (Figure 2b,c).[39] Shortly afterward, Hong et al. reported similar applications with an additional alkyne-tagged glycan.[40] In addition to small-molecule building blocks, Hu et al. recently synthesized and evaluated alkyne-tagged glucose (Figure 2a,b) as an important metabolic probe for interrogating energy demands in live cells and tissues (Figure 2c) and observed heterogeneous glucose uptake patterns with clear cell-to-cell variations in tumor xenograft tissues.[41]

Small-molecule drugs represent an important class of targets for bioorthogonal chemical imaging, since there has been a lack of nonperturbative imaging technologies with high sensitivity and specificity as well as fine spatial and temporal resolution. SRS imaging of alkyne-tagged small-molecule drugs has proven to be effective by evaluating the pharmacokinetics of terbinafine hydrochloride (TH), a FDA approved antifungal drug (Figure 3a).[39] Taking advantage of the deep-tissue imaging capability of


DOI: 10.1021/acs.accounts.6b00210
Acc. Chem. Res. 2016, 49, 1494−1502

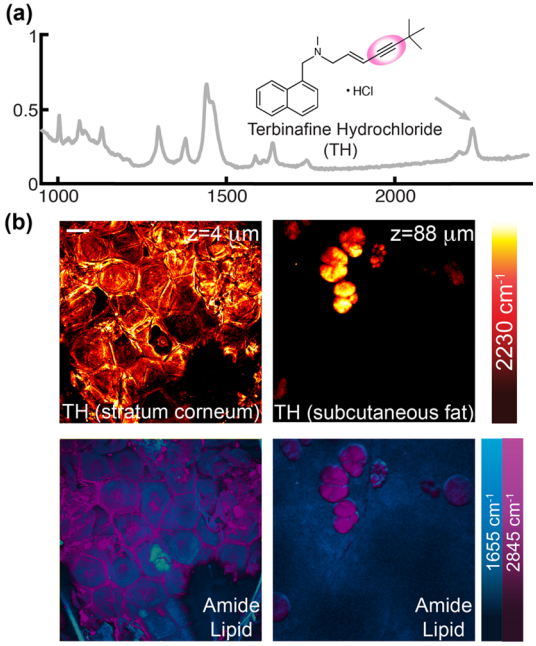


**Figure 3.** SRS imaging of *in vivo* delivery of an alkyne-bearing small-molecule drug, terbinafine hydrochloride (TH), into mouse ear. (a) Spontaneous Raman spectrum of TH. (b) SRS images at selected depths for TH at the alkyne channel and for proteins and lipids at respective label-free amide and lipid channels in mouse ear tissues. Adapted from ref 39. Copyright 2014 Nature Publishing Group. Scale bar: 20 $\mu$m.

SRS, the drug penetration patterns after topical application to mouse ear tissues were revealed. The TH images captured at different depths were all found to highly resemble the lipid but not the protein distributions in the tissues (Figure 3b), suggesting that TH penetrates into tissues through the lipid phase, consistent with its lipophilic nature.[39] This demonstration suggests that SRS tracking of alkyne probes could be a general method for drug imaging after proper alkyne derivatization.

The conjugation system of alkynes can also be slightly enlarged to gain higher SRS signals in a case-by-case manner. Along this line, Lee et al. used SRS imaging of phenyl-diyne tagged cholesterol to assess cholesterol storage in live cells and *Caenorhabditis elegans*,[42] in which phenyl-diyne is found to exhibit an ∼5-times higher signal than a single alkyne in EdU.[39,42] Very recently, Ando et al. synthesized a diyne-tagged sphingomyelin analog and observed a heterogeneous spatial distribution of this probe within *in vitro* raft-like ordered domains by spontaneous Raman.[52] In these cases, the trade-off between the probe size and the achievable SRS signals needs to be carefully balanced.

## 5. SRS IMAGING OF ISOTOPE LABELS

Although alkyne tagging has been proven to be effective and generally applicable, the chemical modifications inevitably introduce a variable degree of alteration to the rates of biosynthesis and metabolism for the tagged biomolecules compared with their natural counterparts. For example, cells incorporate Hpg (homopropargylglycine), an alkyne-bearing methione analogue, about 500 times slower than Met.[34] In this regard, stable isotopes (e.g., deuterium and $C^{13}$) emerge as better vibrational probes, since they only differ from their natural counterparts by neutron numbers and thus closely mimic the corresponding physicochemical properties.

### 5.1. Carbon–Deuterium Probes (C–D)

Carbon–deuterium bonds (C–D) are a type of particularly suited vibrational probe. Chemically, deuterium is a stable isotope of hydrogen without any radioactivity and has an extremely low natural abundance (∼0.016%). Thus, replacing the naturally occurring carbon–hydrogen bonds (C–H) with C–D introduces stable labels with minimum physicochemical alterations. As a matter of fact, the FDA is considering the first approval of a deuterated drug.[53] The kinetic isotope effect is usually negligible for the incorporation and imaging duration of typical experiments. Spectroscopically, C–D bonds also display Raman peaks centered around 2100 $cm^{-1}$ in the desired cell-silent spectral region, shifting the vibrational frequency, $\Omega_{vib}$, away from that of C–H by modulating the reduced mass, $\mu$, in the classical mechanics equation $\Omega_{vib} \propto \sqrt{k/\mu}$. Hence it is not surprising that C–D bonds have been harnessed by Raman spectroscopists and microscopists for decades.

Earlier SRS microscopy of C–D has been convincingly demonstrated for tracking deuterated DMSO penetration in skin tissues and for imaging cellular uptake of deuterated fatty acids.[12,44] In 2013, Wei et al. reported that C–D bonds are especially suitable for tagging amino acids on the stable side-chains and for subsequent SRS imaging of protein synthesis activities.[45] Although the Raman cross-section of C–D is about 30–40 times lower than that of alkynes,[30,39] the particular setting of labeling amino acids by C–D is more ideal, thanks to the enormous number of stable C–H (up to ∼molar in concentration) in multiple amino acids that make up proteins.

*De novo* protein synthesis is the last step of the central dogma, responsible for basic cell survival and proliferation and various cellular responses to environmental stimuli. For instance, this process is closely related to long-term memory formation in neuroscience.[54,55] When deuterated amino acids (*d*-AAs) are supplied to the cell growth medium, they will be metabolically incorporated by cells' natural translational machineries as essential building blocks into newly synthesized proteins (Figure 4a).[45] Therefore, sensitive and specific SRS imaging of newly synthesized proteins enriched with C–D can be achieved by targeting the unique vibrational signature of C–

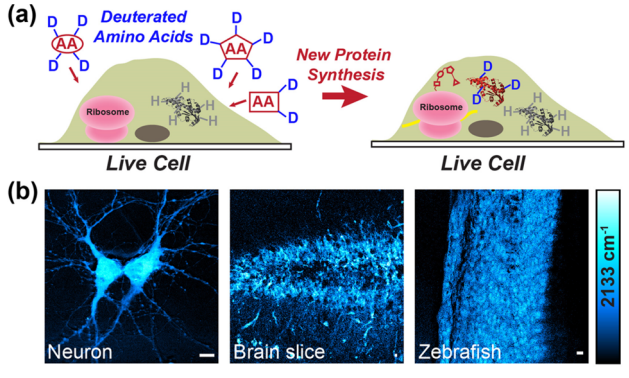


**Figure 4.** SRS imaging of new protein synthesis by metabolic incorporation of deuterated amino acids (*d*-AAs). (a) A cartoon illustrating the metabolic enrichment of *d*-AAs into cells' nascent proteins. (b) SRS images of newly synthesized proteins in live neurons, brain slices, and animals by targeting the C–D vibrational peak. Adapted from ref 46. Copyright 2015 American Chemical Society. Scale bar: 10 $\mu$m.



DOI: 10.1021/acs.accounts.6b00210
*Acc. Chem. Res.* 2016, 49, 1494–1502

D.[45] As a contrast, the unincorporated *d*-AAs in the free amino acid pool are too dilute to be detected. Because of such high signals and biocompatibility offered by *d*-AA labeling, high-quality SRS imaging of protein synthesis has been demonstrated ranging from live mammalian cells and neurons to live brain tissues and to zebrafish and mice *in vivo* (Figure 4b).[45,46] Particularly, fast mapping of protein synthesis activities has been achieved across a large-area of brain tissue (4 mm by 3 mm) within only 2.2 min.[46] Such valuable information on when and where new proteins are actively synthesized in living systems is hard to obtain by other means, such as stable isotope labeling by amino acids in cell culture coupled with mass spectrometry (SILAC-MS).[56]

Moving beyond fatty acids and amino acids, very recently, Hu et al. used $d_9$-choline for imaging choline metabolism in live cells and *C. elegans*,[47] Li et al. implemented $d_7$-glucose for tracing *de novo* lipogenesis,[48] and Alfonso-García et al. adopted $d_{38}$-cholesterol to assess intracellular cholesterol storage.[49] All these applications prove the universal effectiveness and the superb biocompatibility of SRS imaging with C−D tagging.

### 5.2. $^{13}$C Probe

$^{13}$C could also serve as an effective bioorthogonal probe due to its low natural abundance (~1.109%) and its ability to shift the vibrational frequency from the $^{12}$C counterparts. Indeed, $^{13}$C-tagged metabolites have been used in spontaneous Raman for probing cell metabolism.[27,57] Coupling with SRS microscopy, Shen et al. recently demonstrated use of $^{13}$C-tagged phenylalanine for quantitative imaging of proteome degradation.[50] By employing the characteristic ring-breathing modes of endogenous $^{12}$C-phenylalanine ($^{12}$C-Phe) at 1004 cm$^{-1}$ and the metabolically incorporated $^{13}$C-Phe at 968 cm$^{-1}$ as the spectroscopic markers for the old and new proteome, respectively, one can image proteomic degradation by SRS in living cells through ratio maps of $^{12}$C/($^{12}$C + $^{13}$C), in which the total proteome is represented by the sum of $^{12}$C-Phe and $^{13}$C-Phe (Figure 5).[50]

Proteome degradation is a key process to regulate cellular response under pathological or dysfunctional states.[58] Shen et al. applied the method to study the impact of protein aggregation on proteomic degradation of mutant hungtingtin proteins in a mammalian cell model.[50] The obtained results from correlative SRS microscopy and fluorescence imaging of GFP-labeled hungtingtin support the emerging hypothesis that while the diffusive oligomers of aggregation-prone proteins might be toxic by gradually interfering with the proteasome machinery, the formation of inclusion bodies could be neuroprotective by sequestering the diffusive toxic species.[59]

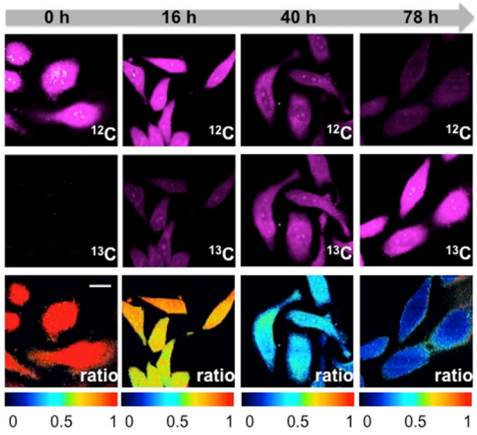


**Figure 5.** SRS imaging of quantitative proteome degradation by metabolical incorporation of $^{13}$C-Phe. Time-dependent images at both $^{12}$C-Phe and $^{13}$C-Phe channels in live HeLa cells are obtained and the ratio maps of $^{12}$C/($^{12}$C+$^{13}$C) show quantitative decay of the pre-existing proteome. Adapted from ref 50. Copyright 2014 John Wiley & Sons, Inc. Scale bar: 20 $\mu$m.

## 6. FUNCTIONAL IMAGING OF DYNAMIC SMALL-MOLECULE METABOLISM IN LIVE SYSTEMS

A distinct advantage for the bioorthognal chemical imaging platform is its superb biocompatibility. Therefore, real-time dynamic analysis is achievable by SRS imaging of vibrational probes to track the intracellular fates of small biomolecules in live systems. Such a capability is beyond the reach of competing techniques, such as click-chemistry followed by fluorescence visualization,[32−38,51] SILAC-MS,[56] and multi-isotope imaging mass spectrometry.[60] To this end, Wei et al. demonstrated the dynamic tracking of cell division after incorporation of either EdU into newly synthesized DNA (Figure 6a)[39] or *d*-AAs into new proteome (Figure 6b).[45] In addition, time-lapse imaging from 10 min to 5 h of active *de novo* protein synthesis on the same set of mammalian cells was also shown (Figure 6c).[46]

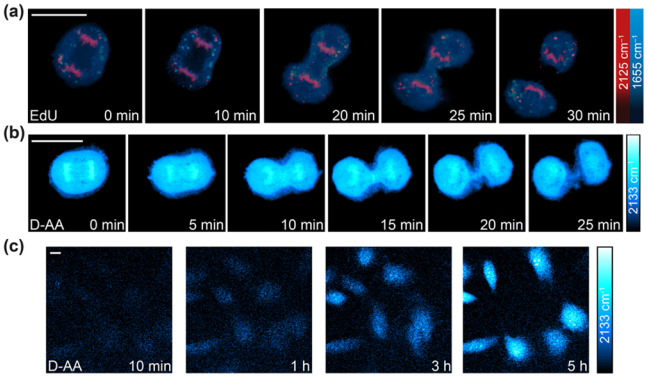


**Figure 6.** Bioorthogonal chemical imaging for the dynamic metabolism of small biomolecules. (a,b) Cell division tracking after incorporated with EdU for newly synthesized DNA (a) and *d*-AAs for newly synthesized proteins (b). Panel a is adapted from ref 39. Copyright 2014 Nature Publishing Group. Panel b is adapted from ref 45. Copyright 2013 National Academy of Sciences. (c) Time-lapse imaging from 10 min to 5 h for protein synthesis with metabolic labeling of *d*-AAs. Adapted from ref 46. Copyright 2015 American Chemical Society. Scale bar: 10 $\mu$m.

## 7. MULTICOLOR BIOORTHOGONAL CHEMICAL IMAGING

A recurring and powerful theme in fluorescence microscopy is the creation of a fluorescent palette, enabling multicolor analysis for separation, colocalization, and interactions. Inspired by the success of fluorescent palettes, a vibrational palette for multicolor bioorthogonal chemical imaging of small biomolecules has also been created. Chen et al. reported isotopic edition of alkynes by modulating the reduced mass of the triple bonds.[43] The resulting vibrational frequencies $\Omega_{vib}$ are shifted from ~2125 cm$^{-1}$ of the original C≡C bond to 2077 cm$^{-1}$ of $^{13}$C≡C and to 2053 cm$^{-1}$ of $^{13}$C≡$^{13}$C. With this novel vibrational palette, previously nondifferentiable small biomolecules bearing the same alkynes could now be spectrally


DOI: 10.1021/acs.accounts.6b00210
Acc. Chem. Res. 2016, 49, 1494−1502

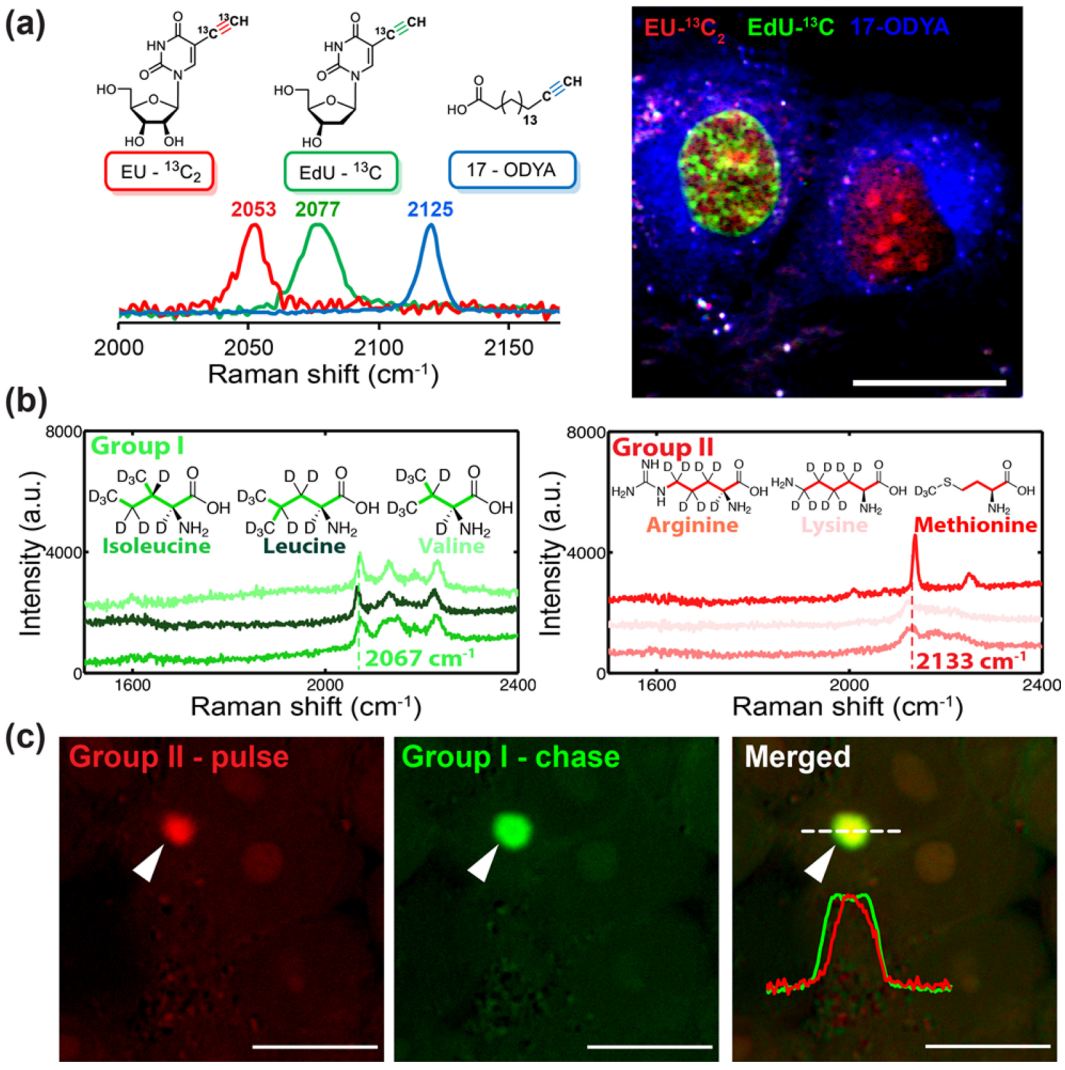


**Figure 7.** Multicolor bioorthogonal chemical imaging. (a) Multicolor SRS imaging of isotope-edited (EdU−$^{13}$C, EU−$^{13}C_2$) and unedited (17-ODYA) alkyne-tagged small biomolecules after metabolic incorporation into new DNA (EdU−$^{13}$C), RNA (EU−$^{13}C_2$), and triglycerides (17-ODYA). Adapted from ref 43. Copyright 2014 American Chemical Society. (b) Subgrouping of *d*-AAs with similar chemical environments. (c) Two-color pulse-chase imaging for the protein aggregation formation of mutant huntingtin proteins by metabolic labeling of two groups of *d*-AAs. Panels b and c adapted from ref 46. Copyright 2015 American Chemical Society. Scale bar: 10 $\mu$m.

separated and imaged simultaneously (Figure 7a),[43] paving the way for multiplex chemical imaging. Since triple bonds present an inherent narrow Raman peak (~14 cm$^{-1}$) and the cell-silent spectral window is rather wide (~1700−2800 cm$^{-1}$), we envision many more vibrational colors could be created upon further chemical manipulations.

In addition to multicolor SRS imaging of isotopic alkynes, Wei et al. performed two-color pulse−chase proteome imaging with *d*-AAs by rationally dividing all *d*-AAs with analogous chemical structures into two subgroups. By this method, aggregation formation of mutant huntingtin proteins was studied by pulse−chase labeling and imaging (Figure 7b,c),[46] demonstrating the ready applicability of the method to untangle complex and dynamic aspects of proteome metabolism. These vibrational palettes created by chemical editing and spectroscopic regrouping empower bioothogonal chemical imaging to be a more versatile platform, allowing for comprehensive study of small biomolecules.

## 8. SUMMARY AND OUTLOOK

SRS microscopy was invented almost a decade ago. These passing years have witnessed the booming advances of SRS microscopy from instrumental developments to biomedical applications. Technically, fast and hyperspectral SRS imaging modalities have been developed by several groups.[61−63] Biomedically, SRS imaging was applied to various studies such as successful delineation of tumor margins.[20] What was relatively lagging behind for the further developments of SRS imaging platform, however, was the contribution from chemistry to create more sensitive and versatile vibrational probes. To this end, we believe the chemical installments of vibrational probes to small biomolecules bridge such a gap between physics/engineering and biomedicine in a timely manner. In retrospect, this evolution path also echoes with the advance of fluorescence microscopy where the imaging probe development gradually becomes the center of the stage and drives innovation forward.

We anticipate the future development for the bioorthogonal chemical imaging platform on several fronts. First, chemical


DOI: 10.1021/acs.accounts.6b00210
*Acc. Chem. Res.* 2016, 49, 1494−1502

derivatization of alkynes (or nitriles) could be expanded to more small biomolecules, such as neurotransmitters, coenzymes, and secondary messengers. Moreover, we expect this platform could be applied to interrogate and potentially offer new biological insights about more complex biological processes including tumor metabolism, long-term memory formation, and neurodegenerative diseases in which the involvement of small molecule metabolism is critical yet hard to study, especially by fluorescence microscopy. Third, thanks to the high nontoxicity of stable isotope labeling, therapeutic imaging and clinical diagnostics, such as intraoperative tumor detection *in vivo* even in humans, could be expected in the near future.

## AUTHOR INFORMATION


### Corresponding Author

*E-mail: wm2256@columbia.edu.


### Notes

The authors declare the following competing financial interest(s): Columbia University has filed a patent application based on this work.

### Biographies

**Lu Wei** received her B.S. degree in Chemistry from Kuang Yaming Honors School, Nanjing University, China, in 2010 and obtained her Ph.D. in Chemistry from Columbia University in 2015. Lu is currently a postdoctoral research scientist at Columbia University. Her research focuses on developing novel nonlinear optical spectroscopy and microscopy and devising new optical bioimaging schemes.

**Fanghao Hu** received his B.S. degree in Chemistry from Wuhan University and is currently a Ph.D. candidate at Columbia University. His research focuses on spectroscopic and chemical development for stimulated Raman scattering imaging in biochemical systems.

**Zhixing Chen** received his B.S. degree from Tsinghua University, China, in 2008. After working as a research assistant in Peking University, he obtained his Ph.D. in chemistry at Columbia University in 2014. Zhixing is currently a postdoctoral researcher at Stanford University. His research interests include novel synthetic chemistry toward small molecules and macromolecules and their applications in the field of bioimaging.

**Yihui Shen** received her B.S. degree in Chemistry from Peking University in 2012. She is currently a Ph.D. candidate in Chemistry at Columbia University and a HHMI International Student Research Fellow. Her research focuses on applying microscopic imaging, including SRS and fluorescence, to provide new biophysical and biochemical insights into metabolic diseases.

**Luyuan Zhang** obtained her Ph.D. in Chemical Physics in 2010 at The Ohio State University. She is currently a postdoctoral research scientist at Columbia University working on imaging abnormal metabolism in morbid animal models. Her research interests are in developing and applying novel nonlinear Raman microscopy for studies of various cellular activities.

**Wei Min** graduated from Peking University, China, with a Bachelor's degree in 2003. He received his Ph.D. in Chemistry from Harvard University in 2008 with Prof. Sunney Xie. After continuing his postdoctoral work in the Xie group, Dr. Min joined the faculty of Department of Chemistry at Columbia University in July of 2010. Dr. Min is currently an Associate Professor there, and his research interests focus on developing novel optical spectroscopy and microscopy technology to address biomedical problems.

## ACKNOWLEDGMENTS

We appreciate helpful discussions with Meng Wang, Colin Nuckolls, Louis Brus, Ann McDermott, Ronald Breslow, Virginia Cornish, Rafael Yuste, Sunney Xie, and Steven Boxer. This work is supported by NIH Director's New Innovator Award (Grant 1DP2EB016573), R01 (Grant EB020892), the US Army Research Office (Grant W911NF-12-1-0594), the Alfred P. Sloan Foundation, and the Camille and Henry Dreyfus Foundation. Y. Shen acknowledges support from HHMI International Student Research Fellowship.

## REFERENCES


(1) Pawley, J. B., Ed. *Handbook of Biological Confocal Microscopy*; Springer: New York, 2006.

(2) Yuste, R., Ed. *Imaging: A Laboratory Manual*; Cold Spring Harbor Press: Cold Spring Harbor, NY, 2010.

(3) Sasic, S., Ozaki, Y., Eds. *Raman, Infrared, And near-Infrared Chemical Imaging*; Wiley: New York, 2011.

(4) Suhalim, J. L.; Boik, J. C.; Tromberg, B. J.; Potma, E. O. The need for speed. *J. Biophotonics* **2012**, *5*, 387−395.

(5) Krafft, C.; Schie, I. W.; Meyer, T.; Schmitt, M.; Popp, J. Developments in spontaneous and coherent Raman scattering microscopic imaging for biomedical applications. *Chem. Soc. Rev.* **2016**, *45*, 1819−1849.

(6) Lane, L. A.; Qian, X.; Nie, S. SERS nanoparticles in medicine: from label-free detection to spectroscopic tagging. *Chem. Rev.* **2015**, *115*, 10489−10529.

(7) Zumbusch, A.; Holtom, G. R.; Xie, X. S. Three-dimensional vibrational imaging by coherent anti-Stokes Raman scattering. *Phys. Rev. Lett.* **1999**, *82*, 4142−4145.

(8) Evans, C. L.; Xie, X. S. Coherent anti-Stokes Raman scattering microscopy: chemical imaging for biology and medicine. *Annu. Rev. Anal. Chem.* **2008**, *1*, 883−909.

(9) Pezacki, J. P.; Blake, J. A.; Danielson, D. C.; Kennedy, D. C.; Lyn, R. K.; Singaravelu, R. Chemical contrast for imaging living systems: molecular vibrations drive CARS microscopy. *Nat. Chem. Biol.* **2011**, *7*, 137−145.

(10) Camp, C. H., Jr.; Cicerone, M. T. Chemically sensitive bioimaging with coherent Raman scattering. *Nat. Photonics* **2015**, *9*, 295−305.

(11) Ploetz, E.; Laimgruber, S.; Berner, S.; Zinth, W.; Gilch, P. Femtosecond stimulated Raman microscopy. *Appl. Phys. B: Lasers Opt.* **2007**, *87*, 389−393.

(12) Freudiger, C. W.; Min, W.; Saar, B. G.; Lu, S.; Holtom, G. R.; He, C.; Tsai, J. C.; Kang, J. X.; Xie, X. S. Label-free biomedical imaging with high sensitivity by stimulated Raman scattering microscopy. *Science* **2008**, *322*, 1857−1861.

(13) Nandakumar, P.; Kovalev, A.; Volkmer, A. Vibrational imaging based on stimulated Raman scattering microscopy. *New J. Phys.* **2009**, *11*, 033026.

(14) Saar, B. G.; Freudiger, C. W.; Reichman, J.; Stanley, C. M.; Holtom, G. R.; Xie, X. S. Video-rate molecular imaging in vivo with stimulated Raman scattering. *Science* **2010**, *330*, 1368−1370.

(15) Min, W.; Freudiger, C. W.; Lu, S.; Xie, X. S. Coherent nonlinear optical imaging: beyond fluorescence microscopy. *Annu. Rev. Phys. Chem.* **2011**, *62*, 507−530.

(16) Cheng, J. -X.; Xie, X. S. *Coherent Raman Scattering Microscopy*; CRC Press: Boca Raton, FL, 2013.

(17) Cheng, J.-X.; Xie, S. X. Vibrational spectroscopic imaging of living systems: emerging platform for biology and medicine. *Science* **2015**, *350*, aaa8870.

(18) Kukura, P.; McCamant, D. W.; Mathies, R. A. Femtosecond stimulated Raman spectroscopy. *Annu. Rev. Phys. Chem.* **2007**, *58*, 461−488.

(19) Lu, F.-K.; Basu, S.; Igras, V.; Hoang, M. P.; Ji, M.; Fu, D.; Holtom, G. R.; Neel, V. A.; Freudiger, C. W.; Fisher, D. E.; Xie, X. S.




DOI: 10.1021/acs.accounts.6b00210
*Acc. Chem. Res.* 2016, 49, 1494−1502

Label-free DNA imaging in vivo with stimulated Raman scattering microscopy. *Proc. Natl. Acad. Sci. U. S. A.* **2015**, *112*, 11624−11629.
(20) Ji, M.; Lewis, S.; Camelo-Piragua, S.; Ramkissoon, S. H.; Snuderl, M.; Venneti, S.; Fisher-Hubbard, A.; Garrard, M.; Fu, D.; Wang, A. C.; Heth, J. A.; Maher, C. O.; Sanai, N.; Johnson, T. D.; Freudiger, C. W.; Sagher, O.; Xie, X. S.; Orringer, D. A. Detection of human brain tumor infiltration with quantitative stimulated Raman scattering microscopy. *Sci. Transl. Med.* **2015**, *7*, 309ra163.
(21) Fu, D.; Yu, Y.; Folick, A.; Currie, E.; Farese, R. V., Jr.; Tsai, T. −H.; Xie, X. S.; Wang, M. C. In Vivo Metabolic Fingerprinting of Neutral Lipids with Hyperspectral Stimulated Raman Scattering Microscopy. *J. Am. Chem. Soc.* **2014**, *136*, 8820−8828.
(22) Fu, D.; Zhou, J.; Zhu, W. S.; Manley, P. W.; Wang, Y. K.; Hood, T.; Wylie, A.; Xie, X. S. Imaging the intracellular distribution of tyrosine kinase inhibitors in living cells with quantitative hyperspectral stimulated Raman scattering. *Nat. Chem.* **2014**, *6*, 614−622.
(23) Liu, B.; Lee, H. J.; Zhang, D.; Liao, C.-S.; Ji, N.; Xia, Y.; Cheng, J.-X. Label-free spectroscopic detection of membrane potential using stimulated Raman scattering. *Appl. Phys. Lett.* **2015**, *106*, 173704.
(24) Lin-Vien, D.; Colthup, N. B.; Fateley, W. G.; Grasselli, J. G. *The Handbook of Infrared and Raman Characteristic Frequencies of Organic Molecules*; Academic Press: Cambridge, MA, 1991.
(25) Ma, J.; Pazos, I. M.; Zhang, W.; Culik, R. M.; Gai, F. Site-specific infrared probes of proteins. *Annu. Rev. Phys. Chem.* **2015**, *66*, 357−377.
(26) Fried, S. D.; Boxer, S. G. Measuring electric fields and noncovalent interactions using the vibrational Stark effect. *Acc. Chem. Res.* **2015**, *48*, 998−1006.
(27) Huang, W. E.; Griffiths, R. I.; Thompson, I. P.; Bailey, M. J.; Whiteley, A. S. Raman microscopic analysis of single microbial cells. *Anal. Chem.* **2004**, *76*, 4452−4458.
(28) van Manen, H. J.; Lenferink, A.; Otto, C. Noninvasive imaging of protein metabolic labeling in single human cells using stable isotopes and Raman microscopy. *Anal. Chem.* **2008**, *80*, 9576−9582.
(29) Yamakoshi, H.; Dodo, K.; Okada, M.; Ando, J.; Palonpon, A.; Fujita, K.; Kawata, S.; Sodeoka, M. Imaging of EdU, an alkyne-tagged cell proliferation probe, by Raman microscopy. *J. Am. Chem. Soc.* **2011**, *133*, 6102−6105.
(30) Yamakoshi, H.; Dodo, K.; Palonpon, A.; Ando, J.; Fujita, K.; Kawata, S.; Sodeoka, M. Alkyne-tag Raman imaging for visualization of mobile small molecules in live cells. *J. Am. Chem. Soc.* **2012**, *134*, 20681−20689.
(31) Lin, L.; Tian, X.; Hong, S.; Dai, P.; You, Q.; Wang, R.; Feng, L.; Xie, C.; Tian, Z. Q.; Chen, X. A bioorthogonal Raman reporter strategy for SERS detection of glycans on live cells. *Angew. Chem., Int. Ed.* **2013**, *52*, 7266−7271.
(32) Prescher, J. A.; Bertozzi, C. R. Chemistry in living systems. *Nat. Chem. Biol.* **2005**, *1*, 13−21.
(33) Grammel, M.; Hang, H. C. Chemical reporters for biological discovery. *Nat. Chem. Biol.* **2013**, *9*, 475−484.
(34) Beatty, K. E.; Liu, J. C.; Xie, F.; Dieterich, D. C.; Schuman, E. M.; Wang, Q.; Tirrell, D. A. Fluorescence visualization of newly synthesized proteins in mammalian cells. *Angew. Chem., Int. Ed.* **2006**, *45*, 7364−7367.
(35) Jao, C. Y.; Salic, A. Exploring RNA transcription and turnover in vivo by using click chemistry. *Proc. Natl. Acad. Sci. U. S. A.* **2008**, *105*, 15779−15784.
(36) Salic, A.; Mitchison, T. J. A chemical method for fast and sensitive detection of DNA synthesis in vivo. *Proc. Natl. Acad. Sci. U. S. A.* **2008**, *105*, 2415−2420.
(37) Jao, C. Y.; Roth, M.; Welti, R.; Salic, A. Metabolic labeling and direct imaging of choline phospholipids in vivo. *Proc. Natl. Acad. Sci. U. S. A.* **2009**, *106*, 15332−15337.
(38) Hang, H. C.; Wilson, J. P.; Charron, G. Bioorthogonal chemical reporters for analyzing protein lipidation and lipid trafficking. *Acc. Chem. Res.* **2011**, *44*, 699−708.
(39) Wei, L.; Hu, F.; Shen, Y.; Chen, Z.; Yu, Y.; Lin, C.; Wang, M. C.; Min, W. Live-cell imaging with alkyne-tagged small biomolecules by stimulated Raman Scattering. *Nat. Methods* **2014**, *11*, 410−412.
(40) Hong, S.; Chen, T.; Zhu, Y.; Li, A.; Huang, Y.; Chen, X. Live-cell stimulated Raman scattering imaging of alkyne-tagged biomolecules. *Angew. Chem., Int. Ed.* **2014**, *53*, 5827−5231.
(41) Hu, F.; Chen, Z.; Zhang, L.; Shen, Y.; Wei, L.; Min, W. Vibrational imaging of glucose uptake activity in live cells and tissues by stimulated Raman scattering. *Angew. Chem., Int. Ed.* **2015**, *54*, 9821−9825.
(42) Lee, H. J.; Zhang, W.; Zhang, D.; Yang, Y.; Liu, B.; Barker, E. L.; Buhman, K. K.; Slipchenko, L. V.; Dai, M.; Cheng, J. X. Assessing cholesterol storage in live cells and C. elegans by stimulated Raman scattering imaging of phenyl-Diyne cholesterol. *Sci. Rep.* **2015**, *5*, 7930.
(43) Chen, Z.; Paley, D.; Wei, L.; Weisman, A.; Friesner, R.; Nuckolls, C.; Min, W. Multicolor live-cell chemical imaging by isotopically edited alkyne vibrational palette. *J. Am. Chem. Soc.* **2014**, *136*, 8027−8033.
(44) Zhang, D.; Slipchenko, M. N.; Cheng, J.-X. Highly sensitive vibrational imaging by femtosecond pulse stimulated Raman loss. *J. Phys. Chem. Lett.* **2011**, *2*, 1248−1253.
(45) Wei, L.; Yu, Y.; Shen, Y.; Wang, W. C.; Min, W. Vibrational imaging of newly synthesized proteins in live cells by stimulated Raman scattering microscopy. *Proc. Natl. Acad. Sci. U. S. A.* **2013**, *110*, 11226−11231.
(46) Wei, L.; Shen, Y.; Xu, F.; Hu, F.; Harrington, J. K.; Targoff, K. L.; Min, W. Imaging complex protein metabolism in live organisms by stimulated Raman scattering microscopy with isotope labeling. *ACS Chem. Biol.* **2015**, *10*, 901−908.
(47) Hu, F.; Wei, L.; Shen, Y.; Min, W.; Zheng, C. Live-cell imaging of choline metabolites through stimulated Raman scattering coupled with isotope-based metabolic labeling. *Analyst* **2014**, *139*, 2312−2317.
(48) Li, J.; Cheng, J.-X. Direct visualization of de novo lipogenesis in single living cells. *Sci. Rep.* **2014**, *4*, 6807.
(49) Alfonso-García, A.; Pfisterer, S. G.; Riezman, H.; Ikonen, E.; Potma, E. O. D38-cholesterol as a Raman active probe for imaging intracellular cholesterol storage. *J. Biomed. Opt.* **2016**, *21*, 061003.
(50) Shen, Y.; Xu, F.; Wei, L.; Hu, F.; Min, W. Live-cell quantitative imaging of proteome degradation by stimulated Raman scattering. *Angew. Chem., Int. Ed.* **2014**, *53*, 5596−5599.
(51) Baskin, J. M.; Prescher, J. A.; Laughlin, S. T.; Agard, N. J.; Chang, P. V.; Miller, I. A.; Lo, A.; Codelli, J. A.; Bertozzi, C. R. *Proc. Natl. Acad. Sci. U. S. A.* **2007**, *104*, 16793−16797.
(52) Ando, J.; Kinoshita, M.; Cui, J.; Yamakoshi, H.; Dodo, K.; Fujita, K.; Murata, M.; Sodeoka, M. Sphingomyelin distribution in lipid rafts of artificial monolayer membranes visualized by Raman microscopy. *Proc. Natl. Acad. Sci. U. S. A.* **2015**, *112*, 4558−4563.
(53) Mullard, A. Deuterated drugs draw heavier backing. *Nat. Rev. Drug Discovery* **2016**, *15*, 219−221.
(54) Hershey, J. W. B., Sonenberg, N., Mathews, M. B., Eds. *Protein Synthesis and Translational Control*; Cold Spring Harbor Laboratory Press: Cold Spring Harbor, NY, 2012.
(55) Martin, K. C.; Barad, M.; Kandel, E. R. Local protein synthesis and its role in synapse-specific plasticity. *Curr. Opin. Neurobiol.* **2000**, *10*, 587−592.
(56) Ong, S. E.; Blagoev, B.; Kratchmarova, I.; Kristensen, D. B.; Steen, H.; Pandey, A.; Mann, M. Stable isotope labeling by amino acids in cell culture, SILAC, as a simple and accurate approach to expression proteomics. *Mol. Cell. Proteomics* **2002**, *1*, 376−386.
(57) Noothalapati Venkata, H. N.; Venkata, N.; Shigeto, S. Stable isotope-labeled Raman imaging reveals dynamic proteome localization to lipid droplets in single fission yeast cells. *Chem. Biol.* **2012**, *19*, 1373−1380.
(58) Goldberg, A. L. Protein degradation and protection against misfolded or damaged proteins. *Nature* **2003**, *426*, 895−899.
(59) Arrasate, M.; Mitra, S.; Schweitzer, E. S.; Segal, M. R.; Finkbeiner, S. Inclusion body formation reduces levels of mutant huntingtin and the risk of neuronal death. *Nature* **2004**, *431*, 805−810.
(60) Zhang, D.-S.; Piazza, V.; Perrin, B. J.; Rzadzinska, A. K.; Poczatek, J. C.; Wang, M.; Prosser, H. M.; Ervasti, J. M.; Corey, D. P.; Lechene, C. P. Multi-isotope imaging mass spectrometry reveals slow protein turnover in hair-cell stereocilia. *Nature* **2012**, *481*, 520−524.


DOI: 10.1021/acs.accounts.6b00210
*Acc. Chem. Res.* 2016, 49, 1494−1502

(61) Ozeki, Y.; Umemura, W.; Otsuka, Y.; Satoh, S.; Hashimoto, H.; Sumimura, K.; Nishizawa, N.; Fukui, K.; Itoh, K. High-speed molecular spectral imaging of tissue with stimulated Raman scattering. *Nat. Photonics* **2012**, *6*, 845−851.
(62) Fu, D.; Holtom, G.; Freudiger, C.; Zhang, X.; Xie, X. S. Hyperspectral imaging with stimulated Raman scattering by chirped femtosecond lasers. *J. Phys. Chem. B* **2013**, *117*, 4634−4640.
(63) Zhang, D.; Wang, P.; Slipchenko, M. N.; Cheng, J.-X. Fast Vibrational Imaging of Single Cells and Tissues by Stimulated Raman Scattering Microscopy. *Acc. Chem. Res.* **2014**, *47*, 2282−2290.



DOI: 10.1021/acs.accounts.6b00210
*Acc. Chem. Res.* 2016, 49, 1494−1502